HHS Public Access

Author manuscript

J Bone Miner Res. Author manuscript; available in PMC 2020 May 09.

Published in final edited form as:

J Bone Miner Res. 2017 March ; 32(3): 654–666. doi:10.1002/jbmr.3023.

Orphan Adhesion GPCR GPR64/ADGRG2 Is Overexpressed in Parathyroid Tumors and Attenuates Calcium-Sensing Receptor-Mediated Signaling

Nariman Balenga[1], **Pedram Azimzadeh**[1], **Joyce A Hogue**[2], **Paul N Staats**[3], **Yuhong Shi**[1], **James Koh**[2], **Holly Dressman**[4], **John A Olson Jr.**[1]

[1]Division of General & Oncologic Surgery, Department of Surgery, University of Maryland School of Medicine, Baltimore, MD, USA

[2]Department of Surgery, Duke University Medical Center, Durham, NC, USA

[3]Department of Pathology, University of Maryland School of Medicine, Baltimore, MD, USA

[4]Department of Molecular Genetics and Microbiology, Duke University, Durham, NC, USA

Abstract

Abnormal feedback of serum calcium to parathyroid hormone (PTH) secretion is the hallmark of primary hyperparathyroidism (PHPT). Although the molecular pathogenesis of parathyroid neoplasia in PHPT has been linked to abnormal expression of genes involved in cell growth (e.g., cyclin D1, retinoblastoma, and β-catenin), the molecular basis of abnormal calcium sensing by calcium-sensing receptor (CaSR) and PTH hypersecretion in PHPT are incompletely understood. Through gene expression profiling, we discovered that an orphan adhesion G protein-coupled receptor (GPCR), GPR64/ADGRG2, is expressed in human normal parathyroid glands and is overexpressed in parathyroid tumors from patients with PHPT. Using immunohistochemistry, Western blotting, and coimmunoprecipitation, we found that GPR64 is expressed on the cell surface of parathyroid cells, is overexpressed in parathyroid tumors, and physically interacts with the CaSR. By using reporter gene assay and GPCR second messenger readouts we identified Gαs, 3',5'-cyclic adenosine monophosphate (cAMP), protein kinase A, and cAMP response element binding protein (CREB) as the signaling cascade downstream of GPR64. Furthermore, we found that an N-terminally truncated human GPR64 is constitutively active and a 15–amino acid–long peptide C-terminal to the GPCR proteolysis site (GPS) of GPR64 activates this receptor. Functional characterization of GPR64 demonstrated its ability to increase PTH release from human parathyroid cells at a range of calcium concentrations. We discovered that the truncated constitutively active, but not the full-length GPR64 physically interacts with CaSR and attenuates

Address correspondence to: Nariman Balenga, PhD, Division of General & Oncologic Surgery, Department of Surgery, Marlene and Stewart Greenebaum Comprehensive Cancer Center, University of Maryland School of Medicine, 655 W. Baltimore St., Room 10-010B, Baltimore, MD 21201, USA. nbalenga@som.umaryland.edu.

Authors' roles: NB and JAO conceived the project, designed and performed the experiments, and co-wrote the manuscript. JAO and HD conducted and analyzed the expression array data. PA performed some of the Western blotting experiments. YS edited the manuscript. JAH, JK, and PNS conducted and evaluated the accuracy and consistency of the immunohistochemistry in tissues.

Disclosures

All authors state that they have no relevant conflicts of interest.

Additional Supporting Information may be found in the online version of this article.

the CaSR-mediated intracellular Ca^{2+} signaling and cAMP suppression in HEK293 cells. Our results indicate that GPR64 may be a physiologic regulator of PTH release that is dysregulated in parathyroid tumors, and suggest a role for GPR64 in pathologic calcium sensing in PHPT.

Keywords

DISORDERS OF CALCIUM/PHOSPHATE METABOLISM; HORMONE REPLACEMENT/ RECEPTOR MODULATORS; CELL/TISSUE SIGNALING; TRANSCRIPTION FACTORS; PTH/VIT D/FGF23

Introduction

Primary hyperparathyroidism (PHPT) is a common endocrine disorder, caused by parathyroid gland neoplasia that variably causes morbidity of the renal, musculoskeletal, cardiovascular, and neural systems.[1] In all cases of PHPT, the neoplastic parathyroid gland(s) hypersecrete parathyroid hormone (PTH), leading to hypercalcemia.[2] The underlying mechanism(s) of PTH hypersecretion are incompletely understood; however, most experimental evidence supports abnormal sensing of extracellular Ca^{2+} concentrations by the calcium-sensing receptor (CaSR), a class C G protein-coupled receptor (GPCR) expressed on the surface of parathyroid chief cells, and the consequent impaired negative feedback to PTH secretion.[3]

CaSR signals through Gαs and Gαi heterotrimeric G proteins to increase the intracellular Ca^{2+}-mediated cytoskeletal remodeling via activation of filamin/RhoA pathway[4] and to reduce cAMP-mediated fusion of secretory granules to the plasma membrane,[5] which ultimately suppress PTH secretion by the parathyroid glands. Several mechanisms of abnormal CaSR biology have been described in parathyroid disorders, including elevated expression of negative regulators of CaSR,[6] inactivating mutations,[7] or reduced expression[8] of CaSR. However, these abnormalities are not universally seen in PHPT, leading to the notion that other mechanism(s) of CaSR dysregulation are involved in the pathogenesis of this disease.

We used a transcriptome screening approach in parathyroid tumors and tissues to identify potential drivers or modifiers of CaSR function.[6] Here, we report that the orphan adhesion G protein-coupled receptor, GPR64/ADGRG2, a receptor with largely unknown function is expressed in normal parathyroid cells and is significantly upregulated in parathyroid tumors collected from patients with PHPT. Adhesion GPCRs form the second largest family of GPCRs and have distinct structural features such as a very large N-terminal segment, which gets autoproteolyzed at the GPCR proteolysis site (GPS). Although their importance in developmental[9] and pathophysiological processes such as diabetes[10] has recently been acknowledged, most of the adhesion GPCRs are still orphans and their signaling pathways and physiological roles are unknown.

GPR64 was initially cloned from a human epididymal cDNA library and because of its apparent absence in other tissues it was named human epididymal-specific protein 6 (HE6).[11] Later, the existence of GPR64 as a two-subunit protein and its epididymal restricted

expression were confirmed in mouse and rat.[12] Global deletion of the seven transmembrane domain (7TM) of mouse GPR64 on X chromosome led to complete infertility in hemizygous males, without showing other significant abnormalities in either females or males.[13] Recently, microarray data showed high expression of GPR64 in Ewing's sarcoma (ES) and some of the lung, melanoma, and kidney cancer cell lines; its knockdown led to reduced tumor growth and metastasis of ES cells in vivo.[14] In a separate study, GPR64 was proposed as a regulator of breast cancer cells adhesion and migration.[15] Together, these studies point to important roles that GPR64 may play in healthy or diseased tissues, if its expression is dysregulated.

In the current study, we provide evidence that GPR64 physically interacts with CaSR and antagonizes CaSR-mediated mobilization of intracellular Ca^{2+} and inactivation of adenylate cyclase. We further show that activation of GPR64 by a 15–amino acid peptide derived from human GPR64 increases secretion of PTH from freshly isolated human parathyroid adenoma cells. Collectively, these findings suggest that this orphan GPCR is important in the parathyroid gland function and may contribute to the abnormal calcium-PTH feedback characteristic of PHPT.

Materials and Methods

Reagents and antibodies

Reagents and antibodies were purchased from the following companies: forskolin (Sigma, St. Louis, MO, USA; #F6886), probenecid (Sigma; #P8761), calcium chloride (Sigma; #21115), H-89 (Cell Signaling Technologies, Beverly, MA, USA; #9844), U0126 (Cell Signaling Technologies; #9903), collagenase (Sigma; #C2674), zeocin (Thermo Fisher Scientific, Waltham, MA, USA; #R25001), Poly-D-Lysine (Sigma; #6407), mouse anti-FLAG (Cell Signaling Technologies; #8146), rabbit anti-HA (Cell Signaling Technologies; #3724), mouse anti-V5 (Thermo Fisher Scientific; #R960–25), rabbit anti-N-terminal epitope of GPR64 (Atlas Antibodies AB, Bromma, Sweden; #HPA001478), mouse anti-CaSR antibody (Thermo Fisher Scientific; #MA1–934), rabbit anti-β-actin (Sigma; #A2066), horseradish peroxidase (HRP)-linked horse anti-mouse IgG (Cell Signaling Technologies; #7076), and HRP-linked goat anti-rabbit IgG (Cell Signaling Technologies; #7074).

Human subjects

Human parathyroid tissue samples were collected and deidentified according to an Institutional Review Board–approved protocol from consented patients undergoing surgery at Duke University and The University of Maryland School of Medicine, as described.[6] Deidentified samples were examined histologically to confirm parathyroid identity.

Plasmids, gene cloning, and mutagenesis

The pcDNA3.1 plasmid encoding the human CaSR variant 1 tagged with a FLAG peptide (pcDNA3.1-FLAG-CaSR) was generated as described.[6] pCRE-Luc plasmid was kindly provided by Evi Kostenis (University of Bonn, Bonn, Germany). pCMV10–3xFLAG-ubiquitin plasmid was a gift from Adriano Marchese (Loyola University, Chicago, IL, USA).

[16] The human GPR64 variant 1 (full-length with 1017 amino acids) was amplified from PFN21A-Halo plasmid (Promega, San Luis Obispo, CA, USA; #FHC11075) by using primers (*for*: TTTAAACTTAAGGCCATGGTTTTCTCTGTCAGGCA and *rev*: CGAGCGGCCGCTTACATTTGCTCAATAAAGTGTAA) and then inserted into pcDNA3.1 plasmid at restriction sites *AflII* and *NotI* (pcDNA3.1-GPR64). Mutations were generated by using Q5 Site-Directed Mutagenesis Kit (New England BioLabs, Ipswich, MA, USA; #E0552S); To construct pcDNA3.1-GPR64ΔNTF, a GPR64 missing the N-terminal fragment (NTF; amino acids 38 to 606), we used pcDNA3.1-GPR64 as template and the following primers (*for*: ACAAGCTTCGGCGTTCTG and *rev*: CGATCCAGCGTAATCTGG). The signal sequence (amino acids 1 to 37) in both GPR64 and GPR64ΔNTF plasmids was replaced by the signal sequence from influenza hemagglutinin (*for*: CATCTTCTGCCTGGTGTTCGCCTACCCATACGATGTTCCAG and *rev*: TAGCTCAGGGCGATGATCGTCTTCATGGTGGCCTTAAGTTTAAAC) to stabilize the surface expression of the receptor in the recombinant system.[17] The N-terminal of receptor was fused to a 3xHA tag (*for*: AGATTACGCTGGATCTTACCCATACGATGTTCCAGATTACGCTGGATCG CTGGAAGAAGATACTGATAATTC and *rev*: GGAACATCGTATGGGTAAGATCCAGCGTAATCTGGAACATCGTATGGGTAGGATGT TACCAGAACGAC) and the C-terminal was fused to V5 tag (*for*: CTCCTCGGTCTCGATTCTACGTAAGCGGCCGCTCGAGTC and *rev*: AGGGTTAGGGATAGGCTTACCCATTTGCTCAATAAAGTGTAAGCTTCCC). A scheme of constructs (pcDNA3.1-SS-3xHA-GPR64-V5 (GPR64) and pcDNA3.1-SS-3xHA-GPR64ΔNTF-V5 (GPR64ΔNTF)) is shown in Fig. 3A. All constructs were verified by complete double stranded sequencing.

Cell culture, generation of stable cell line, and transient transfection

AD-293 (HEK) cells[18] were purchased from Agilent Technologies (Santa Clara, CA, USA; #240085) and cultured in DMEM media (Sigma; #D6429) supplemented with 10% FBS (Sigma; #12303C), 100 U/mL penicillin and 100 μg/mL streptomycin (Thermo Fisher Scientific; #15140–122). HEK cells were transfected with pcDNA3.1-FLAG-CaSR and a clone stably expressing the functional receptor on the surface (HEK-CaSR) was selected in the presence of 0.5 mg/mL zeocin. Cells were starved in DMEM (Thermo Fisher Scientific; #21068028) supplemented with gluta-mine and 1.25 mM Ca^{2+} overnight and assays were performed in the starvation media, unless otherwise mentioned. Transfection was performed with Lipofectamine 2000 transfection reagent (Thermo Fisher Scientific; #11668019) following the manufacturer's instructions. Generation of HEK-FLAG-CB2R/3xHA-GPR55 cells that stably co-express FLAG-tagged cannabinoid 2 receptor and 3xHA-tagged GPR55, was previously described.[18]

Peptide synthesis

Peptides with varying lengths starting at amino acid T607 of human GPR64 were synthesized by GenScript using the solid phase peptide synthesis (SPPS) method followed by deprotecting via Fmoc chemistry. Acetonitrile, water, and Trifluoroacetic acid (TFA) were used for peptide purification leading to >95% purity using a reverse-phase HPLC approach. Peptides were analyzed by HPLC and mass spectrometry to confirm the correct

$[M+H]^+$ and were dissolved in DMSO and stored at –80°C. The sequences are P-11: TSFGVLLDLSR; P-15: TSFGVLLDLSRTSVL; and P-20: TSFGVLLDLSRTSVLPAQMM.

Parathyroid cell isolation and stimulation

Dispersed primary human parathyroid cells were isolated from resected tissues as described.[19] Cells were rested for 1 hour at 37°C in keratinocyte-SFM media (Thermo Fisher Scientific; #37010–022) supplemented with the manufacturer's provided media supplements, antibiotics, and 1.25 mM Ca^{2+}. Cells were then centrifuged and transferred to Keratinocyte SFM (KSFM) media with various concentrations of Ca^{2+}, P-15 peptide, forskolin, and volumetric equivalent of DMSO for 30 min at 37°C. Supernatants were collected by centrifugation at 10,000 *g*, 5 min at 4°C and were stored at –80°C for determination of intact secreted PTH.

Immunohistochemistry, H&E staining, and bright-field imaging

The paraffin-embedded tissues were sectioned (5 μm thick) and immunostained using the Dako EnVision FLEX + Detection system (DAKO, Carpinteria, CA, USA; #K8000). Antigen retrieval was performed by heating at low pH for 20 min and sections were rinsed in Dako wash buffer according to the manufacturer's instructions. Endogenous peroxidase activity was blocked with Peroxidase-Blocking Reagent (10 min) before incubation with rabbit anti-GPR64 antibody at 1:400 for 20 min at room temperature. The primary antibody signal was amplified by EnVision FLEX + Rabbit (LINKER) before incubation with EnVision FLEX/HRP Detection Reagent for 30 min. Finally, sections were stained with 3,3'-diaminobenzidine (DAB) followed by counterstaining with Dako FLEX hematoxylin. Slides were rinsed and mounted in Cytoseal XYL (Thermo Scientific, Waltham, MA, USA). H&E staining was performed as described.[20] The bright field imaging was conducted by 40 oil objective (1.4 NA) on a Nikon Ti-E microscope equipped with 16.2 MegaPixels DS-Ri2 camera. DAB-stained pixels were defined for the Nikon NIS-Elements Basic Research software and were used for calculating the stained area fraction by ROI statistics module, as depicted in Supporting Fig. 5.

Tissue homogenization and RNA/protein isolation

Frozen tissues were homogenized in RNase-free Navy Eppendorf tubes (Next Advance, Averill Park, NY, USA; #NAVYE1-RNA) in a Bullet Blender Storm homogenizer (Next Advance). Protein were isolated by AllPrep DNA/RNA/Protein kit (Qiagen, Valencia, CA, USA; #80004), according to the manufacturer's instruction.

Western blotting

Cell lysates were prepared in radioimmunoprecipitation assay (RIPA) lysis buffer (EMD Millipore, Billerica, MA, USA; #20–188) supplemented with protease inhibitor (Sigma; #P8340) and phosphatase inhibitor (EMD Millipore; #524625) cocktails and were centrifuged at 15,000 *g* for 5 min at 4°C. Supernatants were boiled with reducing sample buffer (Thermo Fisher Scientific; #NP0007 and #NP0009) and 2.5 μg of protein was loaded on 4–12% Bis-Tris gels (Thermo Fisher Scientific; #NP0335) and thereafter transferred to polyvinylidene fluoride (PVDF) membranes. Blocking was performed in TBSTM (TBS +

0.1% Tween-20 + 10% nonfat dry milk) followed by incubation with 1st antibodies in TBSTM (1:2000 for FLAG, HA, V5, and β-actin, 2 hours at room temperature) and (1:500 for GPR64 and CaSR, overnight at 4°C). Bound 1st antibodies were detected with HRP-linked 2nd antibodies against mouse or rabbit IgG at 1:2000 dilution in TBSTM for 2 hours at room temperature. Blots were washed and then developed with ECL Western blotting detection reagents (Amersham, Pittsburgh, PA, USA; #RPN2109). For deglycosylation studies, cleared lysates were incubated with PNGase F (New England BioLabs; #P0708) for 1 hour at 37°C before boiling with sample buffer.

Coimmunoprecipitation assay

Protein-protein interaction in cell membrane was assessed by immunoprecipitation using FLAG Immunoprecipitation kit (Sigma; #FLAGIPT1), as described.[21] In brief, HEK and HEK CaSR cells were transfected with 1 μg pcDNA3.1, pcDNA3.1-SS-3xHA-GPR64-V5, or pcDNA3.1-SS-3xHA-GPR64ΔNTF-V5 plasmids in a six-well plate. Lysis buffer was supplemented with 1 mM $MgCl_2$ and protease inhibitor and cell lysates were either stored at –80°C (Input) or agitated with 20 μL anti-FLAG M2-agarose affinity gel overnight at 4°C. After washing the gels, proteins were eluted by using 3xFLAG peptide (IP) and both Input and IP proteins were deglycosylated with PNGase F at 37°C for 1 hour. Western blotting was performed as described in the Western blotting section above to detect HA, V5, FLAG, and β-actin.

Ubiquitination assay

HEK cells were transfected with pCMV10–3xFLAG-ubiquitin along with either pcDNA3.1, pcDNA3.1-SS-3xHA-GPR64-V5, or pcDNA3.1-SS-3xHA-GPR64ΔNTF-V5 plasmids for 48 hours. Cell lysates were subjected to coimmunoprecipitation with FLAG Immunoprecipitation kit (as described in the Coimmunoprecipitation Assay section above). Glycosylated GPR64 and GPR64ΔNTF were detected in coimmunoprecipitates (IP) and total lysate inputs, using antibodies against HA-tag and V5-tag.

Immunocytochemistry and fluorescence imaging

HEK cells were seeded on glass coverslips coated with Poly-DLysine (50 μg/mL) and were transfected with 0.5 μg plasmids. After overnight starvation, cells were fixed in cold acetone/methanol (1:1 volumetric) for 20 min at –20°C. After washing in PBS, cells were incubated with 5% goat serum in PBS for 1 hour at room temperature as blocking step followed by overnight incubation with rabbit anti-GPR64 (1:200) antibody in 1% bovine serum albumin (BSA) in PBS at 4°C. Cells were then stained with AlexaFluor 594-conjugated goat anti-rabbit (Thermo Fisher Scientific; #A11072) (1:500) for 2 hours at room temperature. Freshly isolated human parathyroid cells were fixed in cold acetone/methanol (1:1 volumetric) for 20 min at –20°C. After washing in PBS, cells were incubated with 5% goat serum in PBS for 1 hour at room temperature as blocking step followed by overnight incubation with isotype control antibodies or rabbit anti-GPR64 (1:200) + mouse anti-CaSR antibodies (1:1000) in 1% BSA in PBS at 4°C. Cells were then stained with AlexaFluor 594-conjugated goat anti-rabbit (Thermo Fisher Scientific; #A11072) (1:500) and AlexaFluor 488-conjugated goat anti-mouse (Thermo Fisher Scientific; #A11017) (1:500) for 2 hours at room temperature. All cells were mounted on ProLong Diamond Antifade Mountant with

DAPI (Thermo Fisher Scientific; #P36971) for nuclear counterstaining. Fluorescence microscopy was conducted by 40 × oil objective (1.4 NA) on a Nikon Ti-E microscope equipped with a 16.2 MegaPixels DS-Ri2 camera and images were analyzed with Nikon NIS-Elements Basic Research software.

CRE reporter gene assays

HEK cells were seeded in white opaque 96-well plates (30,000 cells/well) and were transfected with pCRE-Luc (100 ng/well) along with different doses of empty or GPR64-expressing plasmids. Cells were either left untreated or stimulated with different concentrations of peptides or vehicle for 5 hours at 37°C. Luminescence was measured in a FLEXStation III plate reader (Molecular Devices, Sunnyvale, CA, USA).

Intracellular calcium mobilization assay

Intracellular Ca^{2+} release was measured as described.[22] In brief, HEK and HEK-CaSR cells were transfected with plasmids and seeded at 10,000 cells per well in black, clear-bottom 384-well plates. Forty-eight hours posttransfection, cells were starved in starvation media supplemented with 0.1 mM Ca^{2+} for 5 hours before the assay. Cells were loaded with FLIPR Calcium 5 Assay Kit dye (Molecular Devices) prepared in assay buffer (Hank's balanced salt solution [HBSS] [without Ca^{2+} and Mg^{2+}]+ 0.1 mM Ca^{2+} + 20 mM HEPES + 2.5 mM probenecid at pH 7.4) for 1 hour at 37°C. P-15, Ca^{2+}, and DMSO (vehicle) were prepared at various concentrations in assay buffer. After 20 s baseline reading, compounds were dispensed on a cell plate and changes in fluorescence intensity were measured for another 100 s in a FLEXStation III plate reader (Molecular Devices). Data in HEK-CaSR cells were normalized to the maximum response (elicited by 7.49 mM Ca^{2+} + vehicle) in pcDNA3.1-transfected cells and were plotted as maximum-minimum signal at each concentration. Data from P-15–stimulated HEK cells were normalized to corresponding volumetric concentration of vehicle and were plotted as described for HEK-CaSR cells.

cAMP accumulation assay

HEK and HEK-CaSR cells were seeded in six-well plates and were transfected with 2 μg of plasmids. Forty-eight hours posttransfection, cells were stimulated as follows: HEK-CaSR cells were either kept at normocalcemic condition (1.25 mM Ca^{2+}) or were stimulated with 3 mM Ca^{2+} for 30 min. This was followed by stimulation with either DMSO (vehicle), forskolin (10 μM), or P-15 peptide (100 μM) for an additional 30 min in media containing either 1.25 or 3 mM Ca^{2+}. HCL(0.1 M) was used to stop the stimulation and cleared supernatants were used for cAMP measurement by cAMP complete ELISA kit (Enzo Life Sciences, Farmingdale, NY, USA; #ADI-900–163) and protein measurement by bicinchoninic acid (BCA) method in a Beckman Coulter DTX880 microplate reader (Brea, CA, USA). Data are reported as picomole cAMP per milligrams protein.

Cell surface receptor ELISA

Cells were seeded in 96-well plates and 48 hours posttransfection cells were fixed in 4% paraformaldehyde for 15 min. TBS buffer was used for washing followed by a 30-min blocking in TBSM (TBS + 3% nonfat dry milk). Then cells were incubated with anti-GPR64

(1:500), anti-HA (1:2000), or anti-FLAG (1:3000) antibodies in TBSB (TBS + 3% BSA) for 2 hours at room temperature followed by a 1-hour incubation with HRP-conjugated goat anti-rabbit (1:2000) or HRP-conjugated horse anti-mouse (1:3000) antibodies in TBSM. After washing 5 times with TBS, cells were incubated with TMB (Sigma; #t0440) for 5 min at room temperature. Reaction was stopped by using the same volume of 1 N HCl and absorbance was measured at 450 nm in a Beckman Coulter DTX880 microplate reader.

PTH measurement

Human intact PTH (1–84) in cell supernatants was measured in a colorimetric ELISA assay (Immutopics International, Athens, OH, USA; #60–3000).

Data analysis

Statistical analyses were conducted using appropriate tests for comparisons between two or multiple groups using GraphPad Prism 6.05 (GraphPad, San Diego, CA, USA); $p < 0.05$ was considered to be significant.

Results

GPR64 is expressed in normal parathyroid glands and is upregulated in parathyroid adenomas of PHPT patients

We previously reported a comparative transcriptome analysis of normal human parathyroid using a competitive hybridization against RNA pooled from a broad panel of human cell lines (Stratagene Human Reference RNA), a strategy that revealed a number of parathyroid-enriched genes (GEO accession# GSE83421).[6] In addition to some of the genes known to mediate parathyroid development and function such as *CASR, GCMB, CHGA*, and *PTH* (Fig. 1A, gray bars), we identified *GPR64/ADGRG2* as a gene highly expressed in parathyroid tissue (Fig. 1A, black bar). Expression of *GPR64* in parathyroid glands was confirmed by in silico analysis of publicly available data (GEO accession# GSE10317 and The Human Protein Atlas# ENSG00000173698). Analysis of our array data showed upregulation of GPR64 transcripts in PHPT adenomas compared to normal glands (Fig. 1B).

We confirmed parathyroid tissue expression of GPR64 and evaluated for pathologic expression by immunohistochemical analysis. We proved the specificity of an antibody against GPR64 by using that antibody on epididymis (positive control) and human heart (negative control) and rabbit IgG on human parathyroid (negative control) (Supporting Fig. 1). Specific staining of GPR64 was seen on the surface of parathyroid cells at the cell-cell junctions in normal glands (Fig. 2A). Consistent with the transcriptome data, we found the expression of GPR64 to be highly upregulated in PHPT adenomas compared to normal parathyroid glands (Fig. 2A, B). However, paired normal glands from PHPT patients did not show an upregulation of GPR64 (Fig. 2A, C), suggesting that such differential expression may not be due to dysregulated Ca^{2+}/PTH balance but rather an intrinsic phenotype of adenomatous gland. Western blotting on lysates prepared from normal and tumor parathyroid tissues demonstrated GPR64 as a band at 150 kDa. In line with array and immunohistochemistry results, GPR64 expression was significantly upregulated in tumors compared to normal glands (Fig. 2D, E). However, we did not observe a significant

alteration of CaSR expression (Fig. 2D, F). Also, immunofluorescence staining in dispersed parathyroid adenoma cells showed coexpression of CaSR and GPR64 (Fig. 2G), after confirming the specificity of GPR64 antibody in HEK cells overexpressing GPR64 (Supporting Fig. 2).

GPR64 is processed in HEK cells at its GPCR proteolysis site (GPS)

To investigate the function and signaling cascades emanating from GPR64, we transfected HEK cells with N-terminally HA-tagged and C-terminally V5-tagged full length "human" GPR64 or its mutant that lacks the amino acids N-terminal to the GPS site (GPR64ΔNTF) (Fig. 3A). Similarly truncated "mouse" GPR64 was previously shown to have constitutive activity.[23] Immuno-blotting with HA antibody shows a band of glycosylated GPR64 at 150 kDa and a band of deglycosylated form at 75 kDa, consistent with its predicted molecular weight (Fig. 3B). The V5 tag is detected at 35 kDa in cells transfected with GPR64, proving that this adhesion GPCR mainly gets proteolyzed at GPS site in HEK cells but remains non-covalently bound to the N-terminal fragment. In GPR64ΔNTF-transfected cells V5 tag is detected at 38 kDa due to the co-fusion of 3xHA tag with the rest of the truncated receptor. As predicted, the antibody against N-terminal of GPR64 does not recognize any bands in GPR64ΔNTF-transfected cells. Noteworthy, lysates from GPR64ΔNTF-transfected cells show bands heavier than 38 kDa, which may point to constitutive activity and ubiquitination of this truncated receptor, a phenomenon that is also seen in other adhesion GPCRs.[24] To assess such posttranslational modifications, we tested the conjugation of ubiquitin to these receptors and found that GPR64ΔNTF, unlike GPR64, is ubiquitinated (Fig. 3C).

GPR64 activates the cAMP-PKA-CREB pathway in HEK cells

It was previously shown that mouse GPR64 couples to Gαs signaling cascade and increases the basal level of cAMP.[23] We tested the engagement of this pathway for human GPR64 by measuring the induction of downstream cAMP response element (CRE). Overexpression of full-length GPR64 with high doses of plasmid led to a modest induction of CRE compared to empty vector (Fig. 4A). However, the GPR64ΔNTF showed a significantly higher CRE induction compared to full-length GPR64 or empty vector in a dose-dependent manner (Fig. 4A). Addition of N-terminal HA tag to GPR64 did not alter its incorporation to plasma membrane (Supporting Fig. 3A) and deletion of N-terminal fragment did not significantly change surface expression of GPR64 (Supporting Fig. 3B). These findings support the previously described phenomena of constitutive activity of truncated adhesion GPCRs and the potential inhibitory effect of their N-terminal fragment on downstream signaling cascades.[9]

The extracellular sequence C-terminal to the GPS site (stalk) has been previously shown to activate several adhesion GPCRs including "mouse" GPR64.[23] We synthesized the 11-aa, 15-aa, and 20-aa stalk sequences of human GPR64 (P-11, P-15, and P-20) and observed a concentration-dependent CRE induction in response to these peptides in GPR64ΔNTF-transfected HEK cells (Fig. 4B). Although P-15 and P-20 acted similarly as full agonists (P-15: pEC_{50}: 4.37 ± 0.04; Maximal response: 11.70 ± 0.87 and P-20: pEC_{50}: 4.54 ± 0.11; Maximal response: 9.95 ± 1.65), P-11 showed very low potency and efficacy in this assay (pEC_{50}: 4.10 ± 0.43; Maximal response: 6.11 ± 3.48). Thus, we concluded that the agonistic

features required for full activation of truncated GPR64 are similar between P-15 and P-20 peptides and hence used P-15 for future experiments. We found that P-15 specifically activates full-length GPR64, albeit with lower efficacy compared to truncated GPR64 (Fig. 4C).

A recent study suggested that GPR64 activates the Gαs pathway.[15] We tested the engagement of the Gαs-Calcium pathway downstream of GPR64 via intracellular calcium mobilization assays. HEK cells transfected with control vector, full-length, or truncated GPR64 did not show any increase in cytosolic calcium levels in response to a wide range of concentrations of P-15 (Fig. 4D).

To deepen our understanding of GPR64 signaling pathways, we exploited CRE induction assay as a robust readout. Various pathways can culminate in CRE induction including protein kinase A (PKA)[25,26] and ERK1/2 MAPK enzymes.[27,28] Whereas a specific inhibitor of PKA (H-89) blunted the P-15-triggered CRE induction, the MAP kinase kinase inhibitor (U0126) did not inhibit CRE induction (Fig. 4E). We then investigated the immediate second messenger of the Gαs pathway, cAMP, upstream of PKA. Consistent with CRE assay, we found that P-15 specifically activates GPR64 to produce cAMP and the truncated mutant shows significantly higher cAMP production in both basal and P-15-activated states (Fig. 4F). Together, these results confirm that human P-15 peptide activates human GPR64 to initiate a Gαs-cAMP-PKA-CRE cascade and the N-terminal fragment of GPR64 may act as an intrinsic inhibitor of receptor signaling under normal conditions.

Activation of GPR64 elevates PTH release from tumor parathyroid cells

To examine the role of GPR64 in parathyroid cell function, we treated freshly dispersed human parathyroid adenoma cells with various concentrations of Ca^{2+} and P-15. Calcium stimulation of CaSR suppressed PTH secretion in a dose-dependent manner (Fig. 5A). Interestingly, concomitant activation of GPR64 by P-15 elevated the PTH secretion when cells were kept in media with0.5 and 1.25 mM Ca^{2+} (Fig. 5A). However, this effect was not seen at 3 mM concentration of extracellular Ca^{2+}.

Active GPR64 directly interacts with CaSR

To determine whether the opposing effect of GPR64 on CaSR function is due to direct physical interaction of receptors, we performed coimmunoprecipitation assays. First, we verified the specificity of our assay in HEK (negative control), HEK-FLAG-CaSR (negative control) and HEK-FLAG-CB2R/3xHA-GPR55 cells[21] (positive control) (Supporting Fig. 4). Then, we transfected HEK and HEK-CaSR cells with control or GPR64-expressing plasmids and evaluated physical association of GPR64 with CaSR. After precipitating the FLAG-tagged CaSR with a FLAG-specific antibody from cell lysates, we did not observe any coprecipitation of HA/V5-tagged full-length GPR64 (Fig. 5B). However, we found that 38 kDa GPR64ΔNTF and more strongly its 250 kDa forms coprecipitate with CaSR (Fig. 5B).

We used cell surface–based ELISA to quantify any modulation of CaSR surface expression. We did not find a significant change in cell surface expression of FLAG-tagged CaSR upon coexpression of either GPR64 or GPR64ΔNTF, compared to control plasmid-transfected

cells (Fig. 5C). Overall, these results show that the GPR64 inhibitory effect on CaSR-mediated suppression of PTH release may be due to their heteromerization.

Active GPR64 attenuates the CaSR-mediated intracellular Ca^{2+} release and cAMP suppression

To examine mechanisms by which GPR64 may elevate the PTH secretion in parathyroid cells, we sought to identify possible crosstalk between GPR64 and CaSR at the level of two major second messengers of CaSR pathways, Ca^{2+} and cAMP. Extracellular Ca^{2+} elevated the intracellular Ca^{2+} levels in a concentration-dependent manner in vehicle-treated pcDNA3.1-transfected HEK-CaSR cells (pEC_{50}: 3.535 ± 0.016; Hill slope:2.824 ± 0.235; Maximal response: 101.5 ± 1.177) (Fig. 6A–D). These pharmacological parameters are consistent with potency and cooperativity of CaSR previously reported by others.[29–31] Coadministration of 50 mM P-15 did not alter the CaSR-mediated Ca^{2+} signaling in these cells (pEC_{50}: 3.561 ± 0.015; Hill slope:3.012 ± 0.259; Maximal response: 92.25 ± 1.067). Also, coactivation of CaSR and full-length GPR64 with Ca^{2+} and P-15 did not modulate the intracellular Ca^{2+} signaling significantly (vehicle: pEC_{50}: 3.566 ± 0.010; Hill slope: 2.915 ± 0.159; Maximal response: 101.70 ± 0.762; P-15: pEC_{50}: 3.556 ± 0.015; Hill slope:2.852 ± 0.229; Maximal response: 92.02 ± 1.041) (Fig. 6A–D). However, P-15 significantly reduced the maximal response elicited by CaSR in GPR64ΔNTF-transfected cells without changing its potency or cooperativity (pEC_{50}: 3.555 ± 0.018; Hill slope: 3.485 0.412; Maximal response: 73.34 ± 1.091) (Fig. 6A–F). Moreover, activation of GPR64ΔNTF-transfected cells with vehicle along with Ca^{2+} showed a significant reduction in Ca^{2+} mobilization compared to control-transfected or GPR64-transfected cells (Fig. 6G).

Consistent with previous studies,[32] accumulation of cAMP by adenylate cyclase after forskolin treatment augmented PTH secretion in parathyroid cells (Fig. 7A). Furthermore, while forskolin increased the cAMP level in HEK-CaSR cells kept at normocalcemic condition (1.25 mM Ca^{2+}), activation of CaSR by 3 mM Ca^{2+} suppressed cAMP levels significantly (Fig. 7B). These results confirm the coupling of CaSR to Gαi protein and the consequent negative impact on adenylate cyclase activity and PTH secretion. Activation of CaSR by 3 mM Ca^{2+} significantly reduced the basal cAMP levels in pcDNA3.1-transfected and full-length GPR64-transfected cells (Fig. 7C). However, concomitant treatment with P-15 blocked CaSR effect on cAMP suppression only in GPR64-transfected cells. GPR64ΔNTF increased the cAMP level because of its constitutive activity and although activation of CaSR with 3 mM Ca^{2+} reduced this effect, the cAMP level was still higher than that of cells transfected with empty vector in normocalcemic conditions (Fig. 7C). In addition, concomitant activation of GPR64ΔNTF-transfected cells with 3 mM Ca^{2+} and P-15 peptide resulted in the intracellular cAMP levels higher than in GPR64ΔNTF-transfected cells, which were kept at normocalcemic conditions (Fig. 7C). These results suggest a role for GPR64 in parathyroid adenomas where its activation can oppose the CaSR-mediated Ca^{2+} signaling and adenylate cyclase inactivation and the consequent suppression of PTH secretion.

Discussion

We have shown that the orphan adhesion GPCR, GPR64/ADGRG2 is highly expressed in parathyroid tumors from PHPT patients compared to normal glands and that its extracellular-derived peptide raises PTH secretion from parathyroid adenoma cells. Our data also show that the constitutively active form of GPR64 attenuates the CaSR downstream signaling by multiple pathways and is capable of physical association with the CaSR. Collectively, these data indicate that GPR64 is involved in regulation of PTH secretion by the parathyroid gland and may be involved in the dysregulated feedback of calcium to PTH characteristic of PHPT.

Like other adhesion GPCRs,[33,34] full-length GPR64 gets processed at the GPS site and the resulting NTF protomer remains non-covalently bound to the 7-transmembrane/C-terminal of the receptor. We observed that whereas overexpression of full-length GPR64 modestly induced CRE-luciferase activity, the truncated GPR64 (GPR64ΔNTF) was significantly more constitutively active. This pathway was further potentiated with a 15–amino acid–long peptide synthesized from the C-terminal of GPR64 GPS site. GPR64ΔNTF was more profoundly activated by P-15 than the full-length GPR64, suggesting that the NTF either masks the binding site of the P-15 on GPR64 or conformationally renders the P-15 from its binding site. The presence of a stalk sequence, encompassing the P-15, and the absence of NTF in the truncated form explains its constitutive activity and high responsiveness to P-15. Our observations are consistent with other studies of similar receptors (BAI2/ADGRB2, GPR56/ADGRG1, and CD97/ADGRE5)[24,35,36] showing marginal ligand-independent constitutive activity with wild-type adhesion GPCRs[37] but augmented signaling in the absence of NTF. Although the natural ligand(s) of GPR64 is unknown, our data show that the effect of GPR64 on CaSR signaling depends on the activation state of GPR64 and the presence of the extracellular NTF can hamper that. Notably, the physical interaction of CaSR with the constitutively active/ubiquitinated GPR64ΔNTF might explain the larger impact of P-15–activated GPR64ΔNTF on CaSR-mediated Ca^{2+} and cAMP signaling.

Although our data show an effect of GPR64 on CaSR signaling and PTH secretion by parathyroid adenoma cells, the mechanism(s) by which GPR64 influences PTH secretion by the normal parathyroid gland and its role in abnormal calcium sensing by parathyroid adenoma cells remains unclear. Our data showing that GPR64 directly interacts with CaSR and attenuates its Gαi-mediated cAMP suppression and Gαq-mediated Ca^{2+} mobilization pathways strongly suggests that there is a heteromerization-mediated crosstalk between GPR64 and CaSR, at least in the model HEK-CaSR system. Given the fact that CaSR is known to form homomers,[38] it would be reasonable to investigate whether activated GPR64 affects homomerization and the cooperativity of CaSR protomers going forward. Future studies will also seek to evaluate GPR64 activity in normal parathyroid cells, a challenge given the absence of a relevant parathyroid cell line and the difficulty in obtaining sufficient normal human tissue for *in vitro* studies.

Overexpression of cyclin D1, either by PRAD1 rearrangement or other mechanisms is a well-established cause of parathyroid neoplasia.[39,40] However, the elevated cyclin D1 is only seen in 20% to 40% of parathyroid adenomas.[41] Mouse models of cyclin D1–driven

parathyroid neoplasia that have reduced CaSR expression point to the impact of proliferation as a cause of imbalanced PTH-Ca^{2+} set point.[42] We also found increased expression of cyclin D1 along with GPR64 in PHPT tumors compared to normal glands; however, there were insufficient numbers of samples in this study to draw firm conclusions of association. The relationship between acquired proliferative drive in parathyroid tissue due to cyclin D1 derangements and abnormal calcium sensing beyond alterations in CaSR remain unclear. Whether GPR64 overexpression results from proliferative drive or itself alters the proliferation of parathyroid cells via its antagonistic effects on CaSR signaling remains to be investigated. Recently, elevated expression of GPR64 was shown in metastatic cancer cell lines from different tissues such as bone (Ewing's sarcoma)[14] and breast (MDA-MB231).[15] Whether GPR64 plays any role in parathyroid neoplasia, including carcinoma, is yet to be explored and will likely require a tissue-specific transgenic mouse model.

Currently, parathyroidectomy to remove the causative parathyroid tumor(s) is the only cure for PHPT. Nonsurgical therapeutic approaches to HPT are reserved for patients who cannot be rendered free of their neoplastic parathyroid tissue (eg, parathyroid carcinoma, secondary HPT) or who are unfit for surgery. Current approaches center on calcimimetics (cinacalcet) that act as positive allosteric modulators of CaSR and normalize the serum Ca^{2+} in a significant percentage of patients.[43] Despite their efficacy in this regard, calcimimetics are imperfect in that they do not improve PTH levels durably and do not ameliorate the end-organ effects of excessive PTH in PHPT patients.[44] In contrast, negative allosteric modulators of CaSR (calcilytics) have been tested for other mineral indications; e.g., hypocalcemia and osteoporosis. Although calcilytics resulted in temporal increase of PTH levels and acted as osteoanabolic agent in the ovariectomized rat model of osteopenia,[45] they do not increase bone mineral density in postmenopausal women with osteoporosis, in comparison to patients who received synthetic PTH, teriparatide.[46–48] Both calcimimetics and calcilytics show the promise of CaSR modulating approaches and make relevant the search for additional druggable targets that might affect the calcium-PTH axis in parathyroid tissue. A recent study showed that GPR56/ADGRG1 regulates insulin secretion and proliferation of β cells of human and mouse pancreatic islets via the cAMP-PKA pathway,[10] adding credence to our findings that adhesion GPCRs are involved in physiological functions of endocrine tissues. We believe that GPR64, with its restricted expression in parathyroid, should be further studied as an attractive target for therapeutic intervention in parathyroid disorders.

Supplementary Material

Refer to Web version on PubMed Central for supplementary material.

Acknowledgments

This work was supported by National Institutes of Health Grant R01DK088188 (to JAO), American Cancer Society Institutional Research Grant and Research Starter Grant in Translational Medicine and Therapeutics from PhRMA Foundation (to NB). We thank Kimberly Tuttle for her excellent technical assistance in immunohistochemistry. We express our gratitude to Arya Balenga (Bethesda Elementary School) for drawing the schemes of GPR64 constructs.

References

1. Brown EM. The calcium-sensing receptor: physiology, pathophysiology and CaR-based therapeutics. Subcell Biochem. 2007;45: 139–67. [PubMed: 18193637]
2. Brown EM. Physiology and pathophysiology of the extracellular calcium-sensing receptor. Am J Med. 1999;106(2):238–53. [PubMed: 10230755]
3. Zhang C, Miller CL, Brown EM, Yang JJ. The calcium sensing receptor: from calcium sensing to signaling. Sci China Life Sci. 2015;58(1): 14–27. [PubMed: 25576451]
4. Shoback DM, Thatcher J, Leombruno R, Brown EM. Relationship between parathyroid hormone secretion and cytosolic calcium concentration in dispersed bovine parathyroid cells. Proc Natl Acad Sci U S A. 1984;81(10):3113–7. [PubMed: 6328497]
5. Brown EM, Carroll RJ, Aurbach GD. Dopaminergic stimulation of cyclic AMP accumulation and parathyroid hormone release from dispersed bovine parathyroid cells. Proc Natl Acad Sci U S A. 1977; 74(10):4210–3. [PubMed: 22076]
6. Koh J, Dar M, Untch BR, et al. Regulator of G protein signaling 5 is highly expressed in parathyroid tumors and inhibits signaling by the calcium-sensing receptor. Mol Endocrinol. 2011;25(5):867–76. [PubMed: 21393447]
7. Egbuna OI, Brown EM. Hypercalcaemic and hypocalcaemic conditions due to calcium-sensing receptor mutations. Best Pract Res Clin Rheumatol. 2008;22(1):129–48. [PubMed: 18328986]
8. Farnebo F, Enberg U, Grimelius L, et al. Tumor-specific decreased expression of calcium sensing receptor messenger ribonucleic acid in sporadic primary hyperparathyroidism. J Clin Endocrinol Metab. 1997;82(10):3481–6. [PubMed: 9329389]
9. Hamann J, Aust G, Arac D, et al. International Union of Basic and Clinical Pharmacology. XCIV. Adhesion G protein-coupled receptors. Pharmacol Rev. 2015;67(2):338–67. [PubMed: 25713288]
10. Duner P, Al-Amily IM, Soni A, et al. Adhesion G-protein coupled receptor G1 (ADGRG1/GPR56) and pancreatic beta-cell function. J Clin Endocrinol Metab. 2016:jc20161884.
11. Osterhoff C, Ivell R, Kirchhoff C. Cloning of a human epididymisspecific mRNA, HE6, encoding a novel member of the seven transmembrane-domain receptor superfamily. DNA Cell Biol. 1997; 16(4):379–89. [PubMed: 9150425]
12. Obermann H, Samalecos A, Osterhoff C, Schroder B, Heller R, Kirchhoff C. HE6, a two-subunit heptahelical receptor associated with apical membranes of efferent and epididymal duct epithelia. Mol Reprod Dev. 2003;64(1):13–26. [PubMed: 12420295]
13. Davies B, Baumann C, Kirchhoff C, et al. Targeted deletion of the epididymal receptor HE6 results in fluid dysregulation and male infertility. Mol Cell Biol. 2004;24(19):8642–8. [PubMed: 15367682]
14. Richter GH, Fasan A, Hauer K, et al. G-Protein coupled receptor 64 promotes invasiveness and metastasis in Ewing sarcomas through PGF and MMP1. J Pathol. 2013;230(1):70–81. [PubMed: 23338946]
15. Peeters MC, Fokkelman M, Boogaard B, et al. The adhesion G protein-coupled receptor G2 (ADGRG2/GPR64) constitutively activates SRE and NFkappaB and is involved in cell adhesion and migration. Cell Signal. 2015 12;27(12): 2579–88. [PubMed: 26321231]
16. Marchese A, Benovic JL. Agonist-promoted ubiquitination of the G protein-coupled receptor CXCR4 mediates lysosomal sorting. J Biol Chem. 2001;276(49):45509–12. [PubMed: 11641392]
17. Guan XM, Kobilka TS, Kobilka BK. Enhancement of membrane insertion and function in a type IIIb membrane protein following introduction of a cleavable signal peptide. J Biol Chem. 1992; 267(31):21995–8. [PubMed: 1331042]
18. Balenga NA, Aflaki E, Kargl J, et al. GPR55 regulates cannabinoid 2 receptor-mediated responses in human neutrophils. Cell Res. 2011;21(10):1452–69. [PubMed: 21467997]
19. Shi Y, Hogue J, Dixit D, Koh J, Olson JA Jr. Functional and genetic studies of isolated cells from parathyroid tumors reveal the complex pathogenesis of parathyroid neoplasia. Proc Natl Acad Sci U S A. 2014;111(8):3092–7. [PubMed: 24510902]
20. Balenga NA, Klichinsky M, Xie Z, et al. A fungal protease allergen provokes airway hyper-responsiveness in asthma. Nat Commun. 2015;6:6763. [PubMed: 25865874]

21. Balenga NA, Martinez-Pinilla E, Kargl J, et al. Heteromerization of GPR55 and cannabinoid CB2 receptors modulates signalling. Br J Pharmacol. 2014;171(23):5387–406. [PubMed: 25048571]
22. Yang Z, Balenga N, Cooper PR, et al. Regulator of G-protein signaling-5 inhibits bronchial smooth muscle contraction in severe asthma. Am J Respir Cell Mol Biol. 2012;46(6):823–32. [PubMed: 22281988]
23. Demberg LM, Rothemund S, Schoneberg T, Liebscher I. Identification of the tethered peptide agonist of the adhesion G protein-coupled receptor GPR64/ADGRG2. Biochem Biophys Res Commun. 2015;464(3):743–7. [PubMed: 26188515]
24. Paavola KJ, Stephenson JR, Ritter SL, Alter SP, Hall RA. The N terminus of the adhesion G protein-coupled receptor GPR56 controls receptor signaling activity. J Biol Chem. 2011;286(33):28914–21. [PubMed: 21708946]
25. Zaccolo M cAMP signal transduction in the heart: understanding spatial control for the development of novel therapeutic strategies. Br J Pharmacol. 2009;158(1):50–60. [PubMed: 19371331]
26. Henstridge CM, Balenga NA, Schroder R, et al. GPR55 ligands promote receptor coupling to multiple signalling pathways. Br J Pharmacol. 2010;160(3):604–14. [PubMed: 20136841]
27. Impey S, Obrietan K, Wong ST, et al. Cross talk between ERK and PKA is required for Ca2+ stimulation of CREB-dependent transcription and ERK nuclear translocation. Neuron. 1998;21(4):869–83. [PubMed: 9808472]
28. Sun LS, Quamina A. Extracellular receptor kinase and cAMP response element binding protein activation in the neonatal rat heart after perinatal cocaine exposure. Pediatr Res. 2004;56(6): 947–52. [PubMed: 15470197]
29. Quinn SJ, Ye CP, Diaz R, et al. The Ca2+-sensing receptor: a target for polyamines. Am J Physiol. 1997; 273(4 Pt 1):C1315–23. [PubMed: 9357776]
30. Davey AE, Leach K, Valant C, Conigrave AD, Sexton PM, Christopoulos A. Positive and negative allosteric modulators promote biased signaling at the calcium-sensing receptor. Endocrinology. 2012;153(3):1232–41. [PubMed: 22210744]
31. Hofer AM, Brown EM. Extracellular calcium sensing and signalling. Nat Rev Mol Cell Biol. 2003;4(7):530–8. [PubMed: 12838336]
32. Brown EM, Gardner DG, Windeck RA, Aurbach GD. Relationship of intracellular 3',5'-adenosine monophosphate accumulation to parathyroid hormone release from dispersed bovine parathyroid cells. Endocrinology. 1978;103(6):2323–33. [PubMed: 85548]
33. Ponting CP, Hofmann K, Bork P. A latrophilin/CL-1-like GPS domain in polycystin-1. Curr Biol. 1999;9(16):R585–8. [PubMed: 10469603]
34. Lin HH, Faunce DE, Stacey M, et al. The macrophage F4/80 receptor is required for the induction of antigen-specific efferent regulatory T cells in peripheral tolerance. J Exp Med. 2005;201(10): 1615–25. [PubMed: 15883173]
35. Okajima D, Kudo G, Yokota H. Brain-specific angiogenesis inhibitor 2 (BAI2) may be activated by proteolytic processing. J Recept Signal Transduct Res. 2010;30(3):143–53. [PubMed: 20367554]
36. Ward Y, Lake R, Yin JJ, et al. LPA receptor heterodimerizes with CD97 to amplify LPA-initiated RHO-dependent signaling and invasion in prostate cancer cells. Cancer Res. 2011;71(23):7301–11. [PubMed: 21978933]
37. Liebscher I, Schon J, Petersen SC, et al. A tethered agonist within the ectodomain activates the adhesion G protein-coupled receptors GPR126 and GPR133. Cell Rep. 2014;9(6):2018–26. [PubMed: 25533341]
38. Bai M, Trivedi S, Brown EM. Dimerization of the extracellular calcium-sensing receptor (CaR) on the cell surface of CaR-transfected HEK293 cells. J Biol Chem. 1998;273(36):23605–10. [PubMed: 9722601]
39. Arnold A, Motokura T, Bloom T, et al. PRAD1 (cyclin D1): a parathyroid neoplasia gene on 11q13. Henry Ford Hosp Med J. 1992; 40(3–4): 177–80. [PubMed: 1483873]
40. Motokura T, Arnold A. PRAD1/cyclin D1 proto-oncogene: genomic organization, 5^0 DNA sequence, and sequence of a tumor-specific rearrangement breakpoint. Genes Chromosomes Cancer. 1993;7(2): 89–95. [PubMed: 7687458]

41. Hsi ED, Zukerberg LR, Yang WI, Arnold A. Cyclin D1/PRAD1 expression in parathyroid adenomas: an immunohistochemical study. J Clin Endocrinol Metab. 1996;81(5):1736–9. [PubMed: 8626826]

42. Imanishi Y, Hosokawa Y, Yoshimoto K, et al. Primary hyperparathyroidism caused by parathyroid-targeted overexpression of cyclin D1 in transgenic mice. J Clin Invest. 2001;107(9):1093–102. [PubMed: 11342573]

43. Brown EM. Clinical utility of calcimimetics targeting the extracellular calcium-sensing receptor (CaSR). Biochem Pharmacol. 2010;80(3): 297–307. [PubMed: 20382129]

44. Peacock M, Bilezikian JP, Klassen PS, Guo MD, Turner SA, Shoback D. Cinacalcet hydrochloride maintains long-term normocalcemia in patients with primary hyperparathyroidism. J Clin Endocrinol Metab. 2005;90(1):135–41. [PubMed: 15522938]

45. Kumar S, Matheny CJ, Hoffman SJ, et al. An orally active calcium-sensing receptor antagonist that transiently increases plasma concentrations of PTH and stimulates bone formation. Bone. 2010;46(2):534–42. [PubMed: 19786130]

46. Gowen M, Stroup GB, Dodds RA, et al. Antagonizing the parathyroid calcium receptor stimulates parathyroid hormone secretion and bone formation in osteopenic rats. J Clin Invest. 2000;105(11): 1595–604. [PubMed: 10841518]

47. Nemeth EF, Shoback D. Calcimimetic and calcilytic drugs for treating bone and mineral-related disorders. Best Pract Res Clin Endocrinol Metab. 2013;27(3):373–84. [PubMed: 23856266]

48. Fitzpatrick LA, Dabrowski CE, Cicconetti G, et al. Ronacaleret, a calcium-sensing receptor antagonist, increases trabecular but not cortical bone in postmenopausal women. J Bone Miner Res. 2012;27(2):255–62. [PubMed: 22052452]

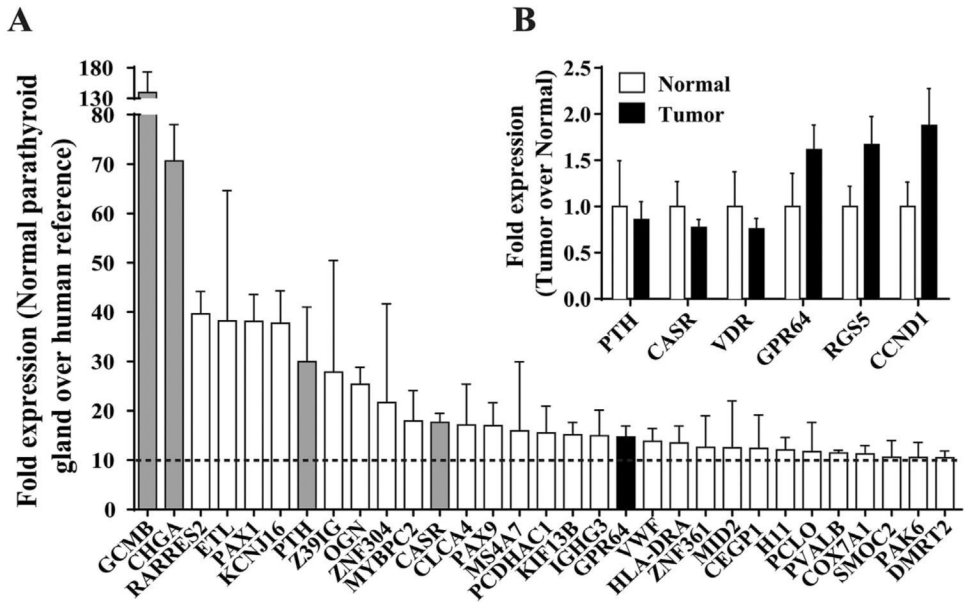

Fig. 1.

Stratagene human reference RNA (pooled from 10 different cell lines) and RNA isolated from six normal parathyroid glands and 25 PHPT parathyroid tumors were competitively hybridized to Operon spotted gene expression array. *(A)* Genes expressed at or higher than 10-fold in normal glands compared to human reference are shown. *(B)* Fold expression of *PTH, CASR, VDR, GPR64, RGS5*, and *CCND1* in PHPT tumors compared to normal glands are shown. Data are mean ± SE. PTH = parathyroid hormone; CASR = calcium-sensing receptor; VDR = vitamin D receptor; RGS5 = regulator of G-protein signaling 5; CCND1 = cyclin D1.

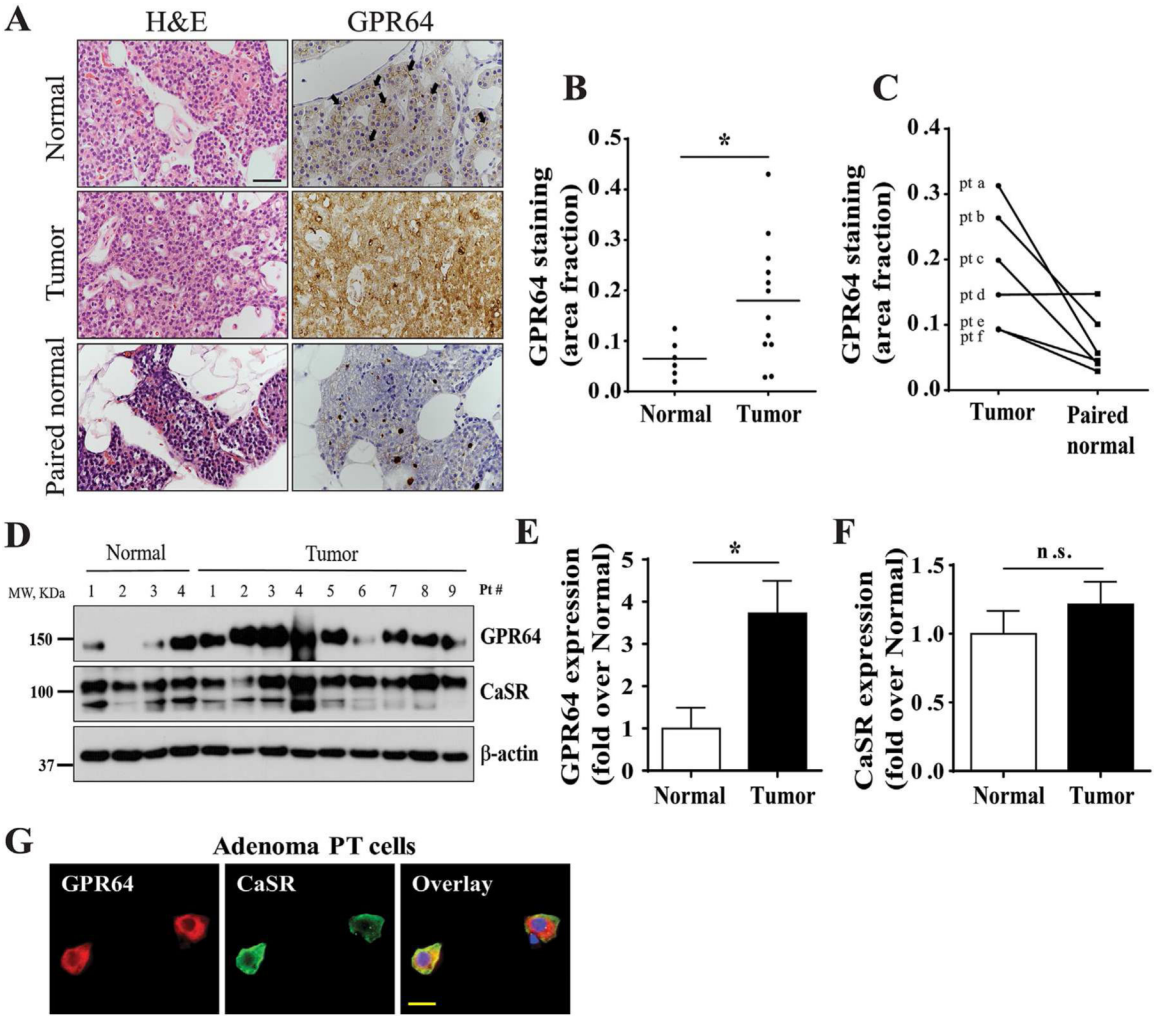

Fig. 2.

(A) Human parathyroid sections from normal glands or tumors and paired normal glands of PHPT patients were stained with an antibody targeted to the N-terminal segment of GPR64 (brown) followed by counterstaining with hematoxylin (purple). Neighboring sections were stained with H&E. Arrows show expression at the cell-cell contacts. Scale bars = 100 μm; original magnification = × 400. *(B)* Comparison of GPR64 staining between parathyroids of healthy controls ($n = 6$) and adenomas of PHPT patients ($n = 12$). $p = 0.0315$ Mann-Whitney U test. (*C*) Comparison of GPR64 staining between parathyroid tumors and normal glands of same PHPT patients ($n = 6$). (*D*) Tissue lysates extracted from normal and tumor parathyroid glands were subjected to immunoblotting with antibodies against CaSR, GPR64, and β-actin. (*E*) Upon normalization to β -actin (as loading control), image analysis of *D* revealed a significant increase in GPR64 expression in tumors compared to normal glands (*$p < 0.05$), while (*F*) expression of CaSR was unchanged. Data shown are mean ± SE. (*G*) Freshly isolated parathyroid adenoma cells were incubated with rabbit anti-GPR64 and mouse anti-CaSR antibodies followed by staining with AlexaFluor-594 conjugated goat anti-rabbit (red) and AlexaFluor-488 conjugated goat anti-mouse antibody (green) and counterstained with DAPI (nuclear, blue). Representative images from four patients are

shown. Scale bar = 20 μm; original magnification = × 400. PT = parathyroid; n.s. = not significant.

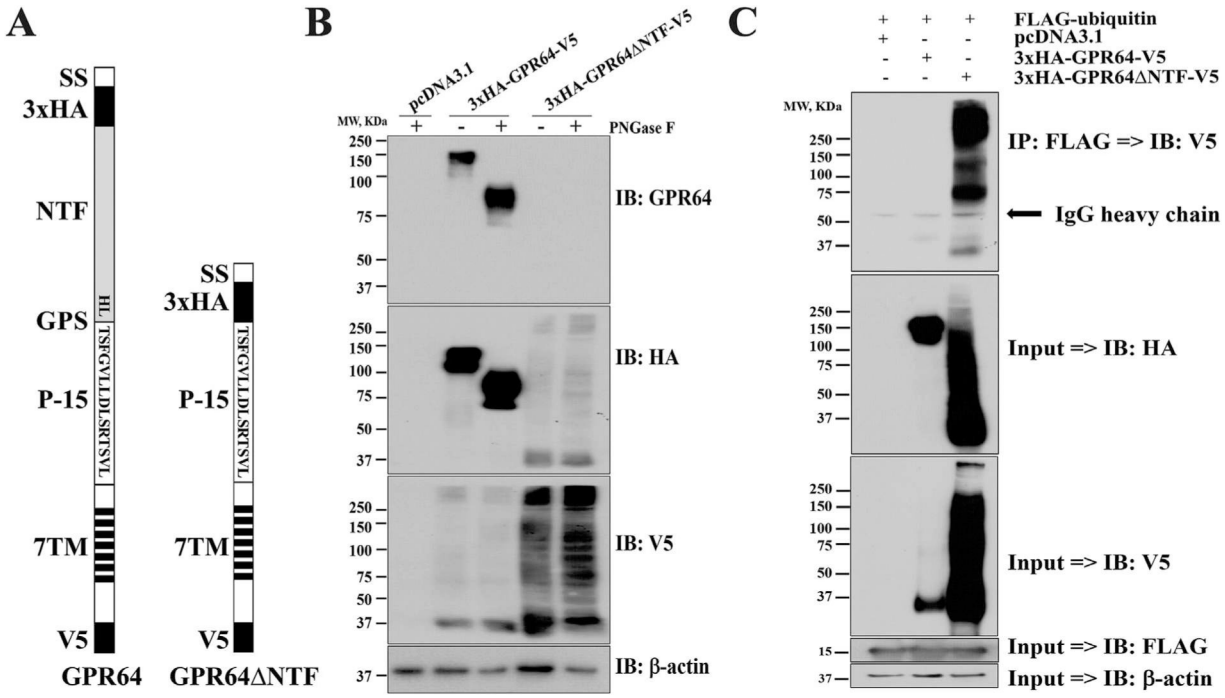

Fig. 3.

(*A*) Schemes of constructs expressing full-length human GPR64 (left) and truncated GPR64 (right) are shown. (*B*) HEK cells were transfected with pcDNA3.1, GPR64, and GPR64ΔNTF plasmids and lysates were either left untreated or incubated with PNGase F for deglycosylation and then subjected to Western blotting. Antibodies against N-terminal of GPR64, HA tag, V5 tag, and β-actin were used. (*C*) HEK cells were transfected with pcMV10–3xFLAG-ubiquitin in combination with pcDNA3.1, GPR64, or GPR64ΔNTF plasmids and cell lysates were either frozen (Input) or incubated with anti-FLAG M2-agarose affinity gels at 4°C overnight. Both Input and eluted samples (IP) were subjected to immunoblotting (IB) with rabbit anti-HA, mouse anti-V5, mouse anti-FLAG, and rabbit anti-β-actin antibodies. Representative membranes from three independent experiments are shown. SS = signal peptide from influenza hemagglutinin gene; 3xHA = triple HA tag; NTF = N-terminal fragment; GPS = GPCR proteolysis site; P-15 = 15–amino-acid–long peptide C-terminal to GPS; 7TM = 7 transmembrane domains; V5 = V5 tag; IB = immunoblotting.

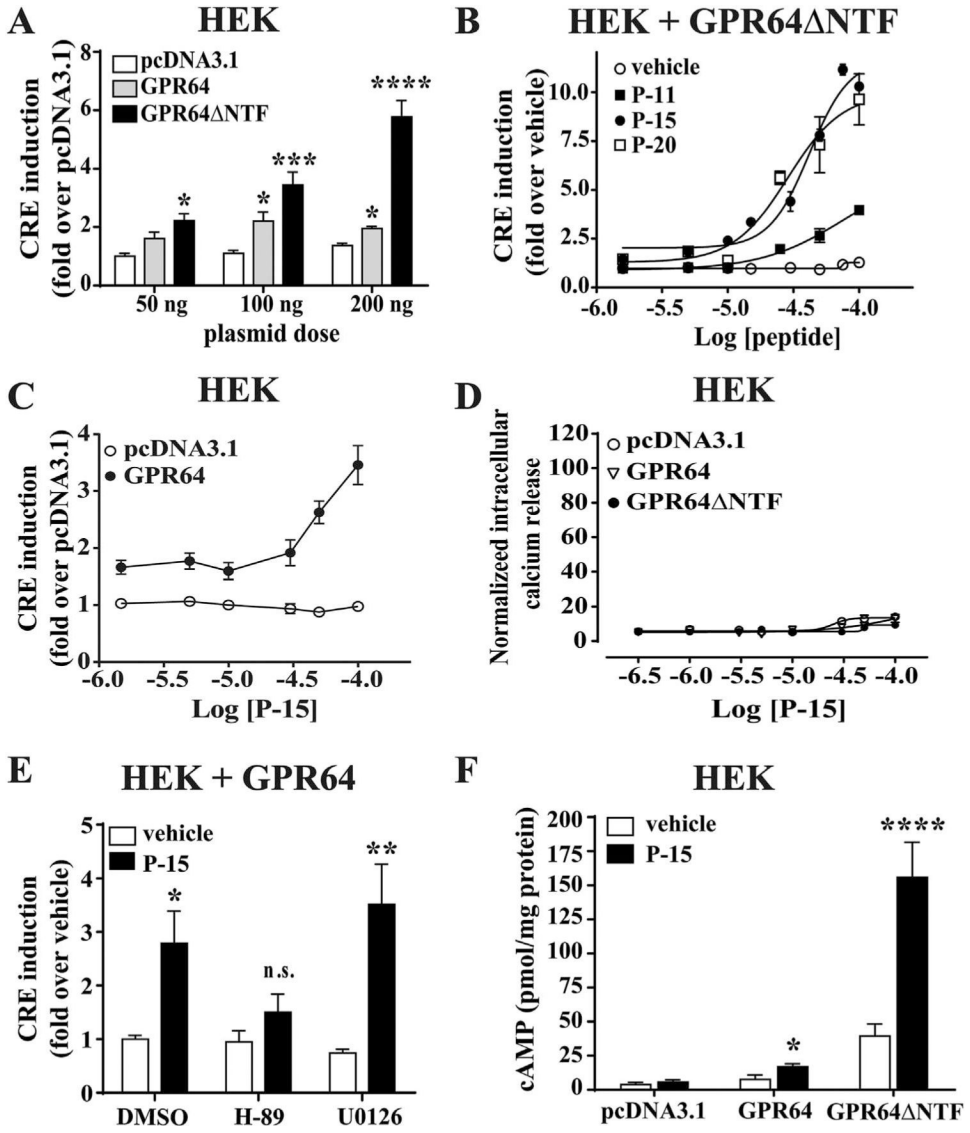

Fig. 4.

(*A*) HEK cells were transfected with pCRE-Luc plasmid along with increasing doses of pcDNA3.1, GPR64, or GPR64ΔNTF. Basal luciferase activity (CRE induction) was measured and data were normalized to the values of cells transfected with 50 ng pcDNA3.1. Data are mean ± SE from six independent experiments conducted in triplicate.*$p < 0.05$, ***$p < 0.001$, ****$p < 0.0001$. (*B*) HEK cells were transfected with pCRE-Luc in combination with 200 ng of GPR64ΔNTF plasmid and were stimulated with increasing concentrations of human GPR64-derived peptides of various length (P-11, P-15, and P-20) or volumetric equivalent of DMSO (vehicle) for 5 hours. Luciferase activity was measured and data were normalized to the values of cells treated with vehicle. Data are mean ± SE from three to four independent experiments conducted in triplicate. (*C*) HEK cells were transfected with pCRE-Luc in combination with 200 ng of pcDNA3.1 or GPR64 plasmids and were stimulated with increasing concentrations of P-15 for 5 hours. Luciferase activity was measured and data were normalized to the values of cells transfected with pcDNA3.1.

Data are mean ± SE from three to four independent experiments conducted in triplicate. (*D*) HEK cells were transfected with 200 ng pcDNA3.1, GPR64, or GPR64ΔNTF plasmids and seeded in 384-well, black, clear-bottom plates. Forty-eight hours posttransfection, cells were loaded with calcium dye and then stimulated with increasing concentrations of P-15 for 2 min in a FlexStation III device. The intracellular calcium mobilization was recorded as change in relative fluorescence units and was used to calculate the maximal-basal signal. Data were normalized to the response elicited by volumetric equivalent of DMSO (vehicle) for each plasmid. Data are mean ± SE from three independent experiments conducted in duplicate. (*E*) HEK cells were transfected with pCRE-Luc and GPR64 and were preincubated with DMSO (vehicle), H-89 (PKA inhibitor, 20 mM), or U0126 (MEK inhibitor, 10 μM) for 1 hour before stimulation with either DMSO or 100 μM P-15 peptide for 5 hours. Luciferase assay data were normalized to vehicle-preincubated, DMSO stimulated cells. Data are mean ± SE from three independent experiments conducted in triplicate.*$p < 0.05$, **$p < 0.01$. (*F*) Forty-eight hours posttransfection with pcDNA3.1, GPR64, or GPR64ΔNTF plasmids, HEK cells were stimulated with DMSO (vehicle) or 100 μM P-15 peptide for 30 min and cAMP accumulation was measured in an ELISA assay at 405 nm. Data were corrected to the protein concentration in samples. Data are mean ± SE from three independent experiments conducted in triplicate.*$p < 0.05$,****$p < 0.0001$. n.s. = not significant.

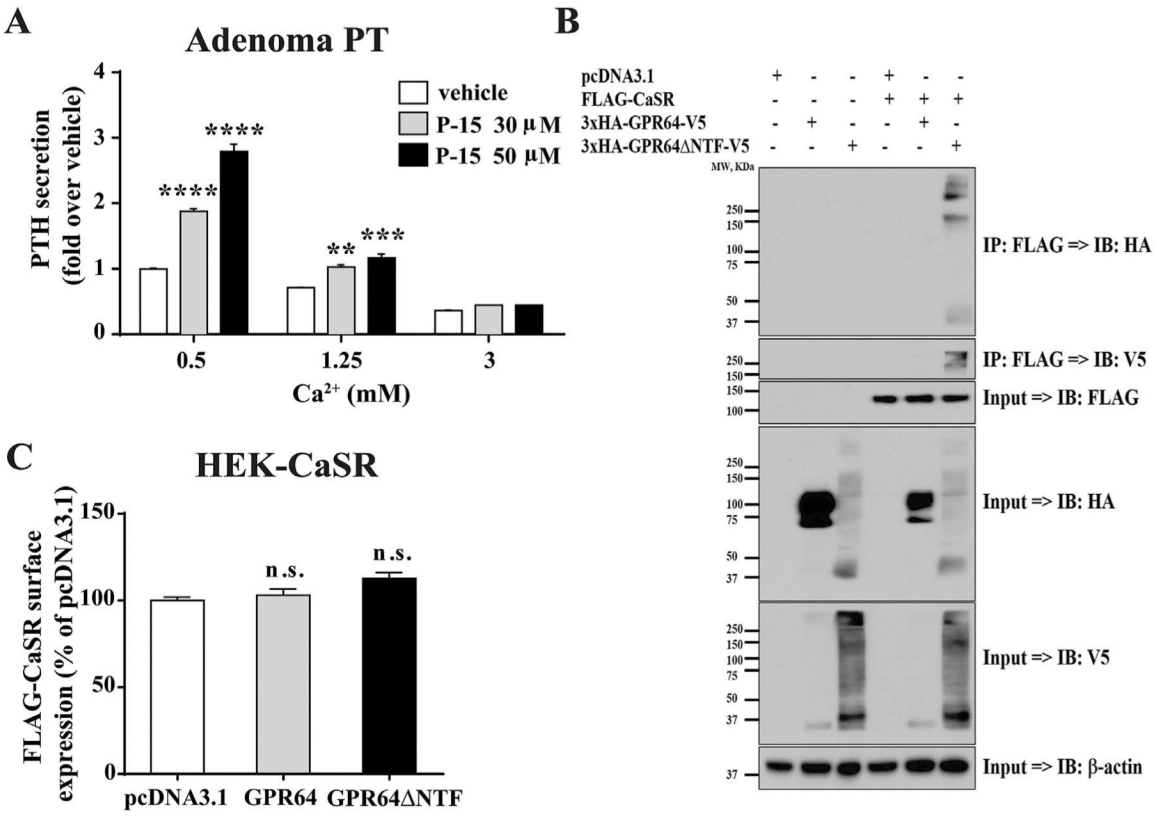

Fig. 5.

(*A*) Freshly isolated human adenoma parathyroid cells were stimulated with increasing concentrations of Ca^{2+} and P-15 or DMSO (vehicle) for 30 min and the concentration of secreted intact PTH was measured by ELISA. Data were normalized to the PTH secretion in vehicle-treated cells cultured in 0.5 mM Ca^{2+}. Data are mean ± SE, representative of five independent experiments. *$p < 0.01$, ***$p < 0.001$, ****$p < 0.0001$. (*B*) HEK and HEK-FLAG-CaSR cells were transfected with pcDNA3.1, GPR64, or GPR64ΔNTF plasmids and cell lysates were either frozen (Input) or incubated with anti-FLAG M2-agarose affinity gels at 4°C overnight. Both Input and eluted samples (IP) were treated with PNGase F and then subjected to IB with rabbit anti-HA, mouse anti-V5, mouse anti-FLAG, and rabbit anti-β-actin antibodies. Representative membranes from three to four independent experiments are shown. (*C*) Surface expression of FLAG-tagged CaSR was measured by quantitative ELISA 48 hours posttransfection with pcDNA3.1, GPR64, or GPR64ΔNTF and data were normalized to the values of empty vector-transfected cells. Data are mean ± SE from three independent experiments conducted in quadruplicate. IB = immunoblotting.

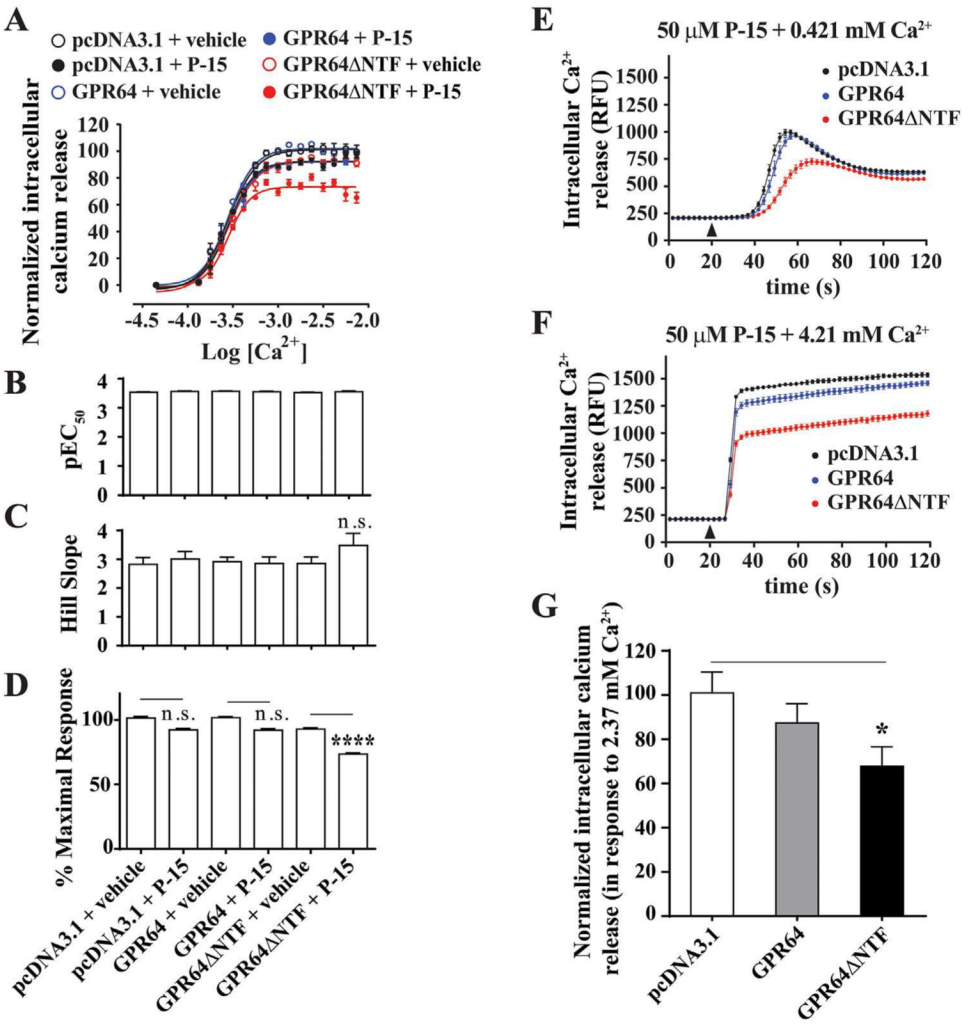

Fig. 6.

HEK-CaSR cells were transfected with pcDNA3.1, GPR64, or GPR64ΔNTF plasmids and seeded in 384-well plates. Forty-eight hours posttransfection cells were loaded with calcium dye and then stimulated with increasing concentrations of Ca^{2+} along with either DMSO (vehicle) or P-15 (50 μM) for 2 min in a FLEXStation III device. The intracellular calcium mobilization was recorded as change in relative fluorescence units and was used to calculate the maximal-basal signal. (*A*) Data were normalized to the response elicited by 7.49 mM Ca^{2+} in vehicle-treated pcDNA3.1-transfected cells. Data are mean ± SE from three independent experiments conducted in triplicate. Potency (pEC50) (*B*), Hill Slope (*C*), and efficacy (% maximal response) (*D*) were derived from the nonlinear dose-response curve fitting performed in GraphPad Prism.****$p < 0.0001$. Time-course of Ca^{2+} mobilization in response to 50 μM P-15 and either 0.421 mM Ca^{2+} (*E*) or 4.21 mM Ca^{2+} (*F*) is shown. Arrowheads show the compound addition time. (*G*) The Ca^{2+} mobilization in response to 2.37 mM Ca^{2+} in the absence of P-15 in transfected cells is shown. Data are mean ± SE from three independent experiments conducted in triplicate.*$p < 0.05$. n.s. = not significant; RFU = relative fluorescence unit; pEC50 = potency.

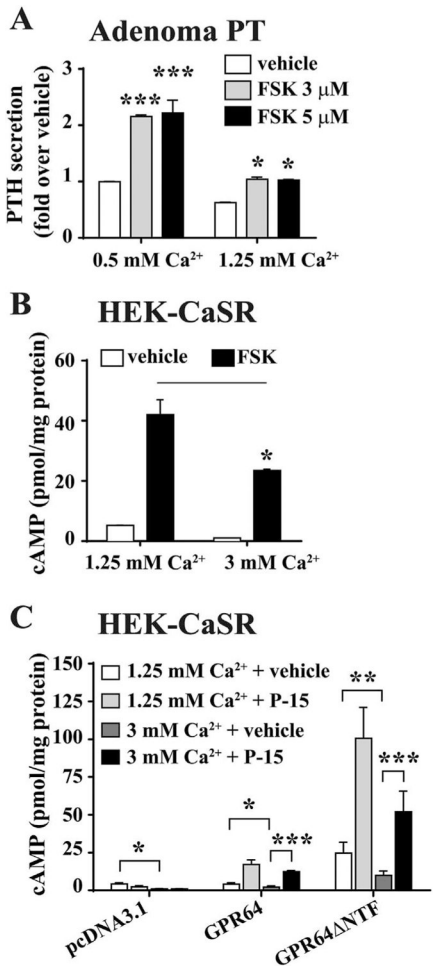

Fig. 7.

(*A*) Freshly isolated human adenoma PT cells were stimulated with increasing concentrations of Ca^{2+} and FSK or DMSO (vehicle) for 30 min and the concentration of secreted intact PTH was measured by ELISA. Data were normalized to the PTH secretion in vehicle-treated cells cultured in 0.5 mM Ca^{2+}. Data are mean ± SE, representative of three independent experiments.*$p < 0.05$,***$p < 0.001$. (*B*) HEK-CaSR cells were stimulated with 1.25 mM or 3 mM Ca^{2+} for 30 min, followed by an additional 30 min incubation with either 10 μM FSK or DMSO (vehicle). cAMP accumulation was measured as in Fig. 4F. Data are mean ± SE representing three independent experiments conducted in duplicate. *$p < 0.05$. (*C*) Forty-eight hours posttransfection with pcDNA3.1, GPR64, or GPR64ΔNTF HEK-CaSR cells were stimulated with either 1.25 mM or 3 mM Ca^{2+} followed by additional 30 min incubation with either 100 μM P-15 or DMSO (vehicle). cAMP accumulation was measured as in B. Data are mean SE representing three independent experiments conducted in duplicate.*$p < 0.05$,**$p < 0.01$,***$p < 0.001$. FSK = forskolin; PT = parathyroid.